Kinematic Coordinates in which Motor Cortical Cells Encode Movement Direction

Robert Ajemian, Daniel Bullock, and Stephen Grossberg[1]

Department of Cognitive and Neural Systems
and
Center for Adaptive Systems[2]

Boston University
677 Beacon St.
Boston, MA 02215

Journal of Neurophysiology, 84, 2191-2203

Technical Report CAS/CNS-TR-98-021
Boston, MA: Boston University

1.This work was supported by the Defense Advanced Research Projects Agency (ONR N00014-92-J-4015), the Defense Advanced Research Projects Agency and the Office of Naval Research (ONR N00014-95-1-0409), the National Science Foundation (NSF IRI-90-00530, and NSF IRI-97-20333), and the Office of Naval Research (ONR N00014-91-J-4100, ONR N00014-92-J-1309, ONR N00014-94-1-0940, and ONR N00014-95-1-0657).

2.The authors would like to thank the following: Robin Amos and Diana Meyers for their valuable assistance in the preparation of the manuscript; Paul Cisek, Mike Cohen, Rajeev Raizada, Matt Giamporcaro, and Steven Wise for helpful comments about the data and model. We also thank Steven Wise for allowing and enabling us to perform original analyses on data from the study of Hocherman and Wise (1991).

ABSTRACT

During goal-directed reaching in primates, a sensorimotor transformation generates a dynamical pattern of muscle activation. Within the context of this sensorimotor transformation, a fundamental question concerns the coordinate systems in which individual cells in the primary motor cortex (MI) encode movement direction. This article develops a mathematical framework that computes, as a function of the coordinate system in which an individual cell is hypothesized to operate, the spatial preferred direction (pd) of that cell as the arm configuration and hand location vary. Three coordinate systems are explicitly modeled: Cartesian spatial, shoulder-centered, and joint angle. The computed patterns of spatial pds are distinct for each of these three coordinate systems, and experimental approaches are described which can capitalize upon these differences to compare the empirical adequacy of each coordinate hypothesis. One particular experiment involving curved motion (Hocherman and Wise 1991) was analyzed from this perspective. Out of the three coordinate systems tested, the assumption of joint angle coordinates best explained the observed cellular response properties. The mathematical framework developed in this paper can also be used to design new experiments that are capable of disambiguating between a given set of specified coordinate hypotheses.

INTRODUCTION

Activity in primary motor cortex (MI) has been implicated in a variety of aspects of movement behavior from control of movement execution to participation in movement planning. Specific examples of MI involvement in the control of kinematic or kinetic attributes of multi-joint movements include established correlations between cell firing rates and the following movement variables: movement direction (Georgopoulos et al. 1982), hand position (Georgopoulos et al. 1984), force (Kalaska et al. 1989; Georgopoulos et al. 1992), hand speed (Schwartz 1992; Ashe and Georgopoulos 1994; Moran and Schwartz 1999a), movement amplitude (Fu et al. 1993), and target direction (Alexander and Crutcher 1990b; Shen and Alexander 1997). Further studies have shown that cell firing rates correlate with aspects of movement planning such as movement preparation (Alexander and Crutcher 1990a; Kettner et al 1996), target sequence information (Carpenter et al. 1997), and rapid motor adaptation (Wise et al. 1998). Cell activity, therefore, shows relations to a multitude of movement variables that span the sensorimotor spectrum.

Since not all MI cells are equally responsive to all these variables, it makes sense to separately investigate distinct components of firing rate modulation. Although force or other movement variables could be analyzed with the methods employed herein, the present analysis focuses on cell response components related to a kinematic variable -- movement direction -- because studies have demonstrated the prevalence and strength of directional coding in MI (Ashe and Georgopoulos, 1994) and because a large literature exists on center-out tasks in which movement direction is the explicitly controlled variable. Still, knowing that cell activity strongly reflects a kinematic movement variable like direction does not specify the nature of the cellular representation: Cartesian spatial coordinates, joint angle coordinates, or muscle length coordinates all might be used to represent movement direction at one neural stage or another.

For the entirety of MI, the supposition of a unique coordinate system in which movement direction is encoded may be inappropriate since a heterogeneity of coordinate systems may exist within a single brain region (Crutcher and Alexander 1990). Indeed it is well-documented that the representations which mediate motor behavior are distributed, often in a graded manner, across extensive, overlapping cortical regions (Mushiake et al. 1991; Fetz 1992; Kalaska and Crammond 1992). Therefore, we restrict our analysis to the single-cell level and ask: how can one analyze

the coordinate system in which an individual cell encodes movement direction? Beyond outlining a general framework for testing alternative coordinate hypotheses, we test three specific coordinate systems — Cartesian spatial, shoulder-centered, and joint angle — with regard to the data of Hocherman and Wise (1991).

THE MODEL AND APPROACH

Preferred directions in an internal space. Georgopoulos et al. (1982) showed that the movement-related activity of many MI cells in the standard center-out task can be represented as:

$$\upsilon(\alpha) = b_0 + b_1 \cos(\omega - \omega_{pd}), \quad (1)$$

where υ is the cell's average firing rate, b_0 is the mean movement-related activity across all directions, b_1 is the amplitude of the direction-dependent modulation of movement-related activity, ω is the movement direction of the hand, and ω_{pd} is the spatial preferred direction or spatial pd, the movement direction in space which elicits the maximal cellular response.

The empirical success of Equation 1 warrants investigating, as one possibility, whether movement direction is represented in a spatial coordinate system. This hypothesis contrasts with some earlier studies where cell activity correlated strongly with muscle force (Evarts 1968; Cheney and Fetz 1980). More recently, Mussa-Ivaldi (1988) demonstrated theoretically that the observed spatial tuning can arise even if a motor cortical cell explicitly controls the time rate of change of multiple muscle lengths. From a diversity of empirical and theoretical studies, no consensus has emerged, and a variety of coordinate interpretations spanning the sensorimotor spectrum have been proposed for understanding directionally-tuned cell activity in MI (Bullock and Grossberg 1988; Mussa-Ivaldi 1988; Caminiti et al. 1990; Schwartz 1992-1994; Sanger 1994; Tanaka 1994; Scott and Kalaska 1997; Zhang and Sejnowski 1999).

A key step to investigating alternative coordinate hypotheses is to distinguish between two types of representation of pds: a *spatial pd* and an *internal pd.* Thus:

Spatial pd: A spatial pd is that hand motion direction, as represented in extrapersonal space, to which a cell will respond maximally during small movements made from a common starting posture. What is meant here by the term 'space' is the coordinate system utilized by the experimentalist in making measurements — typically a Cartesian coordinate system whose axes are aligned with the task space; e.g., the planar surface upon which the monkey performs a center-out task. This coordinate system will henceforth be referred to as Cartesian spatial coordinates.

Internal pd: An internal pd is that movement direction that elicits maximal cell response when represented in whatever coordinates best characterize the cellular-level encoding of movement direction. This 'internal' coordinate system of a cell may be Cartesian spatial coordinates, or it could be some other coordinate system, such as a joint angle or muscle length coordinate system, which is more closely coupled to the biomechanical variables directly affected by the cell through its output connections. Thus, although the spatial pd reflects the internal pd, it is the internal pd that describes a cell's distinctive role in the sensorimotor transformation.

For a well-defined internal coordinate system, mathematical transformations can be used to convert back and forth between a representation of direction in external space and its corresponding representation in the internal space. These transformations are in general posture-dependent — that is, the relationship between directions in the internal space and directions in external space changes as a function of posture. By utilizing the distinctions between a spatial pd and an internal pd as well as the posture-dependent properties of the directional transformations

between the spaces, a vector field method is developed that generates, for a given cell, spatial pd predictions that differ across the workspace as a function of coordinate hypothesis.

METHODS

The model arm. The analysis in this paper assumes a 2-joint or 2-degree-of-freedom (2-DOF) arm moving on a 2-D planar workspace situated within the horizontal plane passing through the shoulder. This model arm, illustrated in Figure 1A, will be referred to as the 2-DOF planar arm. The kinematic equations describing this arm are detailed in the Appendix. A critical feature of the 2-DOF planar arm which simplifies our analysis is that positions map one-to-one to postures.

Modeling internal pds. One complication in adopting Equation 1 as a general model for cell firing rates in center-out type tasks is that spatial pds have been observed to vary with hand position (Caminiti et al. 1990) and, more generally, arm posture (Scott and Kalaska 1997). To account for more of the variance in cell discharge as the center-out task base expands, additional predictor variables (such as hand position) might be added to the regression equation (Ashe and Georgopoulos 1994). Alternatively, a change in the coordinate representation of the variable of interest (Lacquaniti et al. 1995) — in this case, the preferred movement direction — might allow an equation as compact as Equation 1 to account for a larger proportion of the variance. As part of the search for a more generally applicable tuning equation, the 2-DOF planar arm model can be used to construct alternative coordinate systems for the purpose of testing whether Equation 1 — in which a cell's pd is specified once and without regard to the arm's posture — can provide a better data fit *if* the spatial pd is interpreted as a specific instantiation of an underlying and invariant internal pd. A constant internal pd, together with the relevant coordinate transformation, can in principle fully explain the observation of a posture-dependent spatial pd by generating a systematic prediction of the manner in which the spatial pd changes with posture.

To illustrate, suppose that the spatial pd of a cell at some reference posture is direction $\vec{A}$, and that the internal space of a cell is coordinate system $\mathbf{Z}$. Movement direction $\vec{A}$ in space maps to movement direction $\vec{B}$ in coordinate system $\mathbf{Z}$. Now suppose that movements are initiated from a new arm posture. How can we predict the new spatial pd, $\vec{A}'$? Assuming that $\vec{B}$ remains the cell's pd in internal coordinate system $\mathbf{Z}$ at the new arm posture, $\vec{A}'$ can be calculated using the reverse mapping: between directions in coordinate system $\mathbf{Z}$ to directions in external space. In general — for all cases where the internal coordinate system is not identical to external space — $\vec{A}'$ will not be the same as $\vec{A}$, because the transformation between directions in coordinate system $\mathbf{Z}$ and directions in external space depends on posture (i.e., as the posture changes, so does the local relationship between movement directions in the two coordinate systems). This type of coordinate analysis belongs to the branch of mathematics known as differential geometry.

Vector fields of spatial pds. Given a 2-DOF planar arm, hand position maps uniquely to arm posture (which is not the case when the arm possesses redundant degrees of freedom). Thus, determining the spatial pd at every posture is equivalent to uniquely determining the spatial pd at every hand position in the workspace. Specifying a spatial direction and a corresponding magnitude over a field of points in space defines a vector field (in this case, a vector field of spatial pds as in Zhang and Sejnowski 1999). Thus, an internal pd in a particular coordinate system implies a vector field of spatial pds. To illustrate, plots of vector fields of spatial pds were constructed under the assumption of each of three internal coordinate systems for a sample cell whose spatial pd is $60°$ at a reference posture, as indicated in Figure 1A.

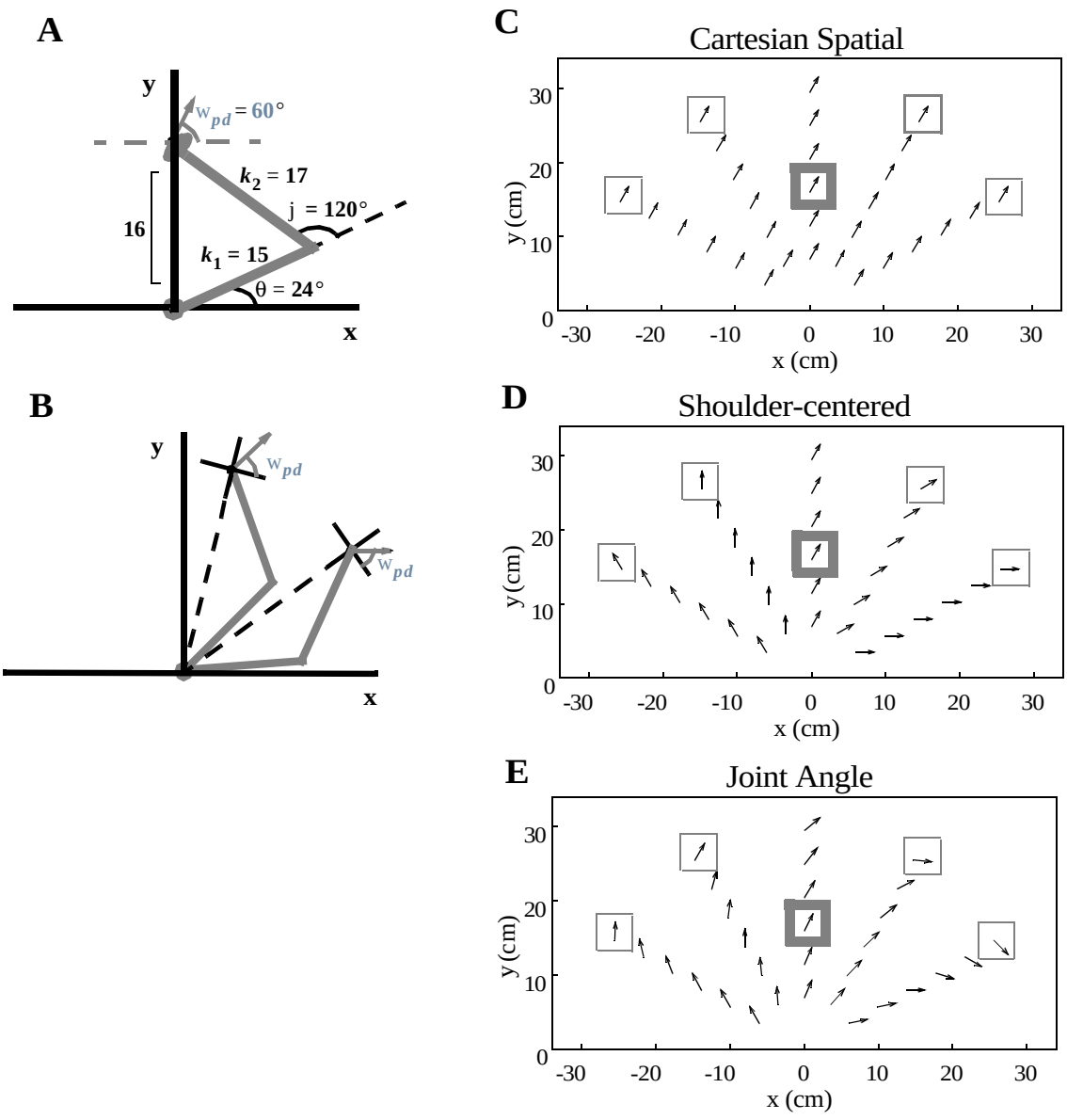

Figure 1. A) Model arm and spatial pd at the reference posture. The model describes a two-link planar arm controlled by shoulder flexion/extension and elbow flexion/extension. k_1 denotes the length of the upper arm segment and k_2 denotes the length of the lower arm segment. A shoulder rotation (denoted by θ) of $24°$ and an elbow rotation (denoted by φ) of $120°$ specify the reference posture of the arm. At this posture, which places the hand at the point (0,16), the spatial pd of the sample cell is $60°$. All lengths are given in cm. B) Illustration of shoulder-centered coordinates. The spatial pd is defined relative to a coordinate system that is aligned with respect to the shoulder-hand axis. As the hand moves about the workspace, the spatial pd rotates the same amount as the shoulder-hand axis rotates. In C, D, and E, vector fields of spatial pds are constructed for the sample cell under the assumption of each of the three internal coordinate systems. For each plot, the vector in the center of the workspace, surrounded by the thick grey box, corresponds to the spatial pd at the reference posture which, by definition, is identical for the three coordinate hypotheses. Using the direct sampling paradigm, one can, on a cell-by-cell basis, compare spatial pd predictions at a small number of other postures — such as those enclosed by the thin grey boxes — to the observed spatial pds to compare the goodness of fit of the alternative coordinate systems.

Cartesian spatial coordinates. The simplest vector field arises when the internal coordinate system in which a cell encodes movement direction is the same Cartesian spatial coordinate system in which spatial pds are measured. Psychophysical evidence (Morasso 1981) suggests that movement planning may occur in this coordinate system. Spatial pds for this case will not vary with posture because the spatial pd at the reference posture is also the cell's internal pd; in other words, the identity transformation converts between the two representations of direction. Figure 1C shows this constant-direction vector field of spatial pds. The magnitude of each vector is unity; the Appendix describes how magnitudes are determined. For this and subsequent vector field plots, information regarding the direction but not magnitude of the vectors is provided.

A vector at a given point in these vector field plots represents the cell's expected spatial pd *if the center-out task were performed with that point as the movement origin*. Because it is impractical to map out a cell's vector field of spatial pds by performing the center-out task as many times as there are arrows on the simulation plots, alternative testing methods are described later.

Shoulder-centered coordinates. One axis important for many mammals is the line between the proximal and distal end of a limb; e.g. between the shoulder and the hand (Maioli and Lacquaniti 1988). Psychophysical studies (Soechting and Flanders 1989; Flanders et al. 1992) have suggested the existence of a shoulder-referenced spatial coordinate system, and cell data have been interpreted in terms of a shoulder-referenced intrinsic coordinate system (Caminiti et al. 1990, 1991; Tanaka 1994). In consideration of these observations, suppose as shown in Figure 1B that a cell's spatial pd is computed in a mobile Cartesian spatial reference frame, one axis of which is aligned with the axis connecting the shoulder to the hand. As the shoulder-hand axis rotates (due to rotations at the shoulder and/or elbow joints), the cell's spatial pd rotates by an equivalent amount. Thus, the rotational transformation converts between representations of direction in the two spaces. Figure 1D plots the variable-direction vector field of spatial pds generated for the sample cell with a constant pd in shoulder-centered coordinates. Specifications for generating this vector field are contained in the Appendix.

Joint angle coordinates. An MI cell may encode movement in a joint angle coordinate system that represents a later stage in the sensorimotor transformation from spatial coordinates to muscle activations. Psychophysical studies on motor adaptation (Shadmehr and Mussa-Ivaldi 1994; Gandolfo et al. 1995) have implicated joint-based representations. Mussa-Ivaldi (1988) suggested that MI cell activity could be a linear function of the rate of multiple muscle length changes. More recently, Scott and Kalaska (1997) introduced a joint angle interpretation of MI cell activity, and our interpretation is similar to theirs.

Suppose that at the reference posture, (θ_R, φ_R), a cell possesses a spatial pd, ω_{pd}. Using the inverse of the Jacobian of the kinematic transformation from joint angle coordinates to spatial coordinates, this spatial direction can be converted to a direction in joint angle space. Upon moving to a new posture, the Jacobian can be used to convert the joint angle direction back to a spatial pd. Since the Jacobian is posture-dependent, application of the inverse Jacobian followed by application of the forward Jacobian evaluated at a *new* posture is not equivalent to operating with the identity transformation; the composite transformation will result in a new spatial pd. The mathematical details of constructing this vector field are contained in the Appendix.

An intuitive explanation of what it means for a cell to possess an internal pd in a joint angle coordinate system is as follows. Suppose the internal pd for a cell is:

$$\begin{bmatrix} \dot{\theta}_{pd} \\ \dot{\phi}_{pd} \end{bmatrix} = \begin{bmatrix} 1 \\ 3 \end{bmatrix} \quad (2)$$

where $\dot{\theta}_{pd}$ and $\dot{\phi}_{pd}$ correspond to the relative shoulder and elbow components of the preferred velocity vector in joint angle space. Such a cell responds maximally to directions of coordinated 2-joint motions produced when the elbow rotation rate is three times the shoulder rotation rate. Depending upon the posture, the spatial movement direction that corresponds to this movement direction in joint angle space (i.e., this joint synergy) will vary. Figure 1E depicts the vector field of spatial pds generated for the sample cell with a constant pd in joint angle coordinates.

Global description of vector fields. These three vector fields simulated for a sample cell clearly differ from one another. Is there any simple way to classify the differences in their structure without comparing vectors in the alternative vector fields one by one for each cell? The *curl* of a vector field is a local measure of the rotational tendency of vector field flow; that is, a measure at a point of how much the vectors rotate in the neighborhood of that point. Observing how the curl changes across the workspace helps to explicate the global structure of a vector field. Below we present the distinct curls for each of the three classes of vector fields described above. The mathematical details of the derivations are reported in the Appendix.

Cartesian spatial coordinates: Cartesian spatial internal pds imply that the spatial pds do not change. Hence, there is no oriented flow to the vector field, and its curl is everywhere zero.

Shoulder-centered coordinates: Vector fields generated under the assumption of this coordinate system yield:

$$\mathbf{curl}(x, y) = \frac{-\cos \omega_{pd}(x_R, y_R)}{r} \quad (3)$$

where $\omega_{pd}(x_R, y_R)$ is the spatial pd of the cell at the reference posture, and r is the distance of the hand from the shoulder. The inverse dependence on r indicates that the rotational tendency of vectors diminishes at more distal portions of the workspace.

Joint angle coordinates: For a cell tuned to an invariant direction in joint angle space, this internal pd can be written as a normalized joint angle velocity vector ('*' denotes normalization):

$$\begin{bmatrix} \dot{\theta}^*_{pd} \\ \dot{\phi}^*_{pd} \end{bmatrix}$$

where $\dot{\theta}^*_{pd}$ denotes the shoulder component of the preferred joint synergy and $\dot{\phi}^*_{pd}$ denotes the elbow component. The curl value for the vector field of such a cell is:

$$\mathbf{curl}(x, y) = 2\dot{\theta}^*_{pd} + \dot{\phi}^*_{pd} \quad (4)$$

This curl is a non-zero constant (no dependence on hand position or arm posture). Thus, vectors in this vector field rotate (in sharp contrast to Cartesian spatial coordinates) and their rotational tendency is uniform throughout the workspace (in sharp contrast to shoulder-centered coordinates). The constant value depends only on the joint synergy to which the cell is tuned.

Utility of Vector Fields. Measuring the curl experimentally is problematic since it is a local measure whose accurate estimation at multiple points would require a high resolution sampling of the workspace that may be difficult to accomplish in practice. Nonetheless, for any pair of candidate coordinate systems, computation of the curl indicates whether the two coordinate systems give rise to vector fields of similar or disparate structure, and thus whether they are empirically distin-

guishable. Based on this fact, two distinct methods for experimentally disambiguating between distinguishable vector field structures are now described: **direct field sampling** and **indirect field sampling**.

Direct field sampling. This method determines spatial pds at several different workspace locations and then, using a least mean square analysis, compares the results with those predicted by the different coordinate hypotheses. For example, spatial pd predictions at the locations indicated by the thin-lined boxes in Figure 1C, D, and E can be compared to determine which coordinate system provides the best fit. Knowledge of the vector field structure can optimize the discriminatory efficacy of the direct field sampling paradigm because it enables workspace sampling that focuses on those locations that give rise to very different predictions for the coordinate systems being evaluated. For 2-D planar arm movements, no experiment has been performed that directly sampled the workspace in the manner suggested above, although Caminiti et al. (1990) and Scott and Kalaska (1997) have performed experiments based on this concept (see Discussion).

Indirect field sampling. Another method relies on investigating cortical activity during long, curved movements that sweep broadly across the workspace, thereby visiting many postures and implicitly sampling a cell's vector field of spatial pds over a single trajectory. The pattern of movement-related activity registered by a cell along multiple such paths determines the cell's *trajectory-selectivity* or its tendency to respond preferentially to certain types of trajectories. A cell's trajectory-selectivity, if any, can serve as the signature for a specific coordinate system.

Equation 1 was initially applied only locally and only to movements of constant spatial direction. For long, curved trajectories the spatial movement direction of the hand varies continuously and the hand position or arm posture can change significantly as well. Schwartz (1992) demonstrated that, for the traversal of sinusoidal trajectories, the activity of many MI cells varied continuously as a function of the continuously changing movement direction in accord with Equation 1. That is, Equation 1 held even when the neural recordings were taken during movements in which the movement direction markedly varied, provided that there was an appropriate temporal lead between the cell firing rate and the corresponding hand movement direction. A similar finding was made regarding a spiral tracing task in Moran and Schwartz (1999b).

On the basis of these and other findings which suggest that directional control is an important aspect of movement control, we hypothesize that cells will respond in continuous accord with the principles of broad directional tuning (as embodied by tuning curves such as the cosine model) in arbitrary movement tasks. Thus, the movement-related temporal discharge pattern of a cell during an arbitrary movement trajectory can be modeled by: (1) breaking the trajectory into a large number of small, essentially linear, path segments; (2) determining the movement direction within a given bin; and (3) applying Equation 1 to each of these path segments. These steps will determine the direction-dependent component of cell activity over the course of a movement path.

To complete the determination of the temporal response profile, we note that MI cell response for trained movements with unimodal speed profiles often takes the form of a phasic pulse or burst-like response. Many generative hypotheses are consistent with this shape. As the focus of this article is not on explicating the specific shape of the response, but on understanding how variations in cell response arise as a function of the directional characteristics of the movement path taken by the hand, we simply assume a generic burst-like shape for cell response in our simulations. Therefore, to determine the temporal response profile, the directional component of cell activity (as determined in steps 1-3 above) is modulated by a generic Gaussian that embodies the phasic response properties of many MI cells. The Gaussian modulation is a fixed component

of cell response used identically for all paths and coordinate assumptions, and it introduces no bias. Simulations showed that the precise form of the response envelope (which included different pulse shapes as well as the constant function) does not alter the results on trajectory-selectivity. A determination of trajectory-selectivity indicates that a cell responds preferentially to certain movement paths, and this path-dependent response depends upon the variable directional component of cell response and not upon the fixed modulatory component.

Averaging the activity over all the bins of a movement path determines the mean firing frequency over the course of the entire movement. Thus, the average firing rate, $\bar{v}$, of a cell over the course of an arbitrary trajectory can be expressed as:

$$\bar{v} = \left(\frac{1}{T}\right)\sum_{i=1}^{n} G(i)\left(b_0 + b_1\cos\left(\omega(i) - \omega_{pd}(i)\right)\right)\Delta t_i \qquad (5)$$

where i denotes the bin number, Δt_i denotes the duration of bin i, G denotes the modulation of the burst-like activity by a Gaussian, and $T = \sum_{i=1}^{n} \Delta t_i$ denotes the total movement time. Note that since the movement direction, ω, and spatial pd, ω_{pd}, are written as functions of the bin number (i.e., the position along the movement path), both are interpreted as varying as a function of hand position or arm posture. Therefore, not only does the movement direction in general change as the hand traverses a curved path, but so too may the cell's spatial pd.

Hocherman and Wise (1991). The data of Hocherman and Wise (1991) is now analyzed within the framework of indirect field sampling for the purpose of evaluating the adequacy of the three internal coordinate hypotheses. That study investigated the correlation between individual motor cortical cell activity and the curvature type of end-effector motion. Briefly, a monkey was trained (by use of intermediate via points between the movement origin and target locations) to make movements of different curvature types from an origin point to each of three equidistant targets spaced at intervals of 30 degrees. Both the arm and the targets were constrained to lie on a 2-D planar surface. The three movement types consisted of clockwise arcs, straight lines, and counter-clockwise arcs; a movement of each curvature type was made to each of the three targets for a total of nine distinct trajectories which are numerically labeled in Figure 2. Unconstrained return movements were also part of the protocol so even though the targets were concentrated in a $60°$ wedge, movement directions did span the entire $360°$ of the angular continuum.

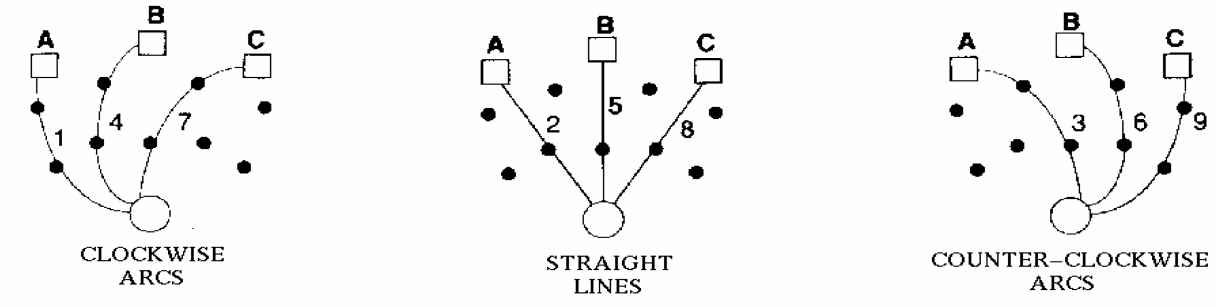

Figure 2. Three types of movement curvature in the experiment of Hocherman and Wise (199). A movement of each curvature type was made to each of the three targets (A,B,C). Comparisons were made for movements to the same target to see if a cell responded preferentially to movements of one specific curvature type across all targets.

Cell activities were recorded in the arm area of MI both before and during the movements. (In the actual experiment, cell recordings occurred in several different epochs, but we only simulate activity for a single movement-related epoch, which corresponds closely to their 'late movement epoch'.) In the study, a neuronal modulation index, M_j, was used as a normalized measure of a cell's average movement-related activity for path j and was computed with the equation:

$$M_j = \frac{A_j - R}{A_{MAX} - R}, \tag{6}$$

where A_j is the cell's average activity over movement path j, R is the cell's resting discharge rate, and A_{MAX} is the cell's average discharge rate over that movement path (of the nine) for which the cell is maximally active. An M value close to 1 means a cell is highly active for that path, while an M value close to 0 means the cell is largely inactive. Cells were classified as trajectory-selective for a certain curvature type if they were preferentially active for movements of that curvature type (see the Appendix). For example, a cell that was clockwise trajectory-selective exhibited higher levels of activity for the clockwise trajectories (labeled in Figure 2 as 1, 4, and 7) than for its straight or counter-clockwise movement counterparts. Similar definitions held for classifying cells as straight trajectory-selective or counter-clockwise trajectory-selective.

Using the method of indirect field sampling, we simulated the experiment of Hocherman and Wise (1991) by (1) computing each model cell's modulation index for all of the nine movement paths using their normalization procedures, (2) classifying model cells using their classification criteria, and (3) generating cellular temporal response profiles. A model cell was identified by its spatial pd at the reference posture; the population of model cells consisted of 360 cells, one for each degree of the angular continuum. Simulation details are found in the Appendix.

RESULTS

Simulations of trajectory-selectivity. A key discovery of Hocherman and Wise (1991) was a strong tendency for cells to respond preferentially to movements of the curved trajectory types. Illustrations of the results of the original experiment are given in Figures 3A and 3C which show the percentages of trajectory-selective cells for each trajectory type using the *strict* (3A) and *relaxed* (3C) criteria to classify cells.

For the simulations run under the assumptions of Cartesian spatial, shoulder-centered, and joint angle coordinates, there were, respectively, 181, 156, and 135 task-related model cells out of a total of 360 model cells. The spatial pds of these cells at the reference posture were almost entirely contained in the $0° - 180°$ range since the movement directions required to reach the targets also exist in that range. Plots in Figure 3B and 3D depict the percentages of cells which were trajectory-selective for each trajectory type using each classification criterion. Under the assumptions of both Cartesian spatial coordinates and shoulder-centered coordinates, the vast majority of the trajectory-selective model cells, 100% and 68% respectively, were trajectory-selective for the straight trajectory type when the strict classification criterion was used; using the relaxed criterion, the percentages were 98% and 69%. These simulation results are not consistent with the data where the vast majority of trajectory-selective cells are of the two curved movement types. Under the assumption of joint angle coordinates, however, the majority of model cells were — like MI cells — trajectory-selective for the curved trajectories. Furthermore, the percentages of

all three types of trajectory-selective cells using the joint angle model correspond well with the data for both classification schemes, as can be seen by comparing the graphs.

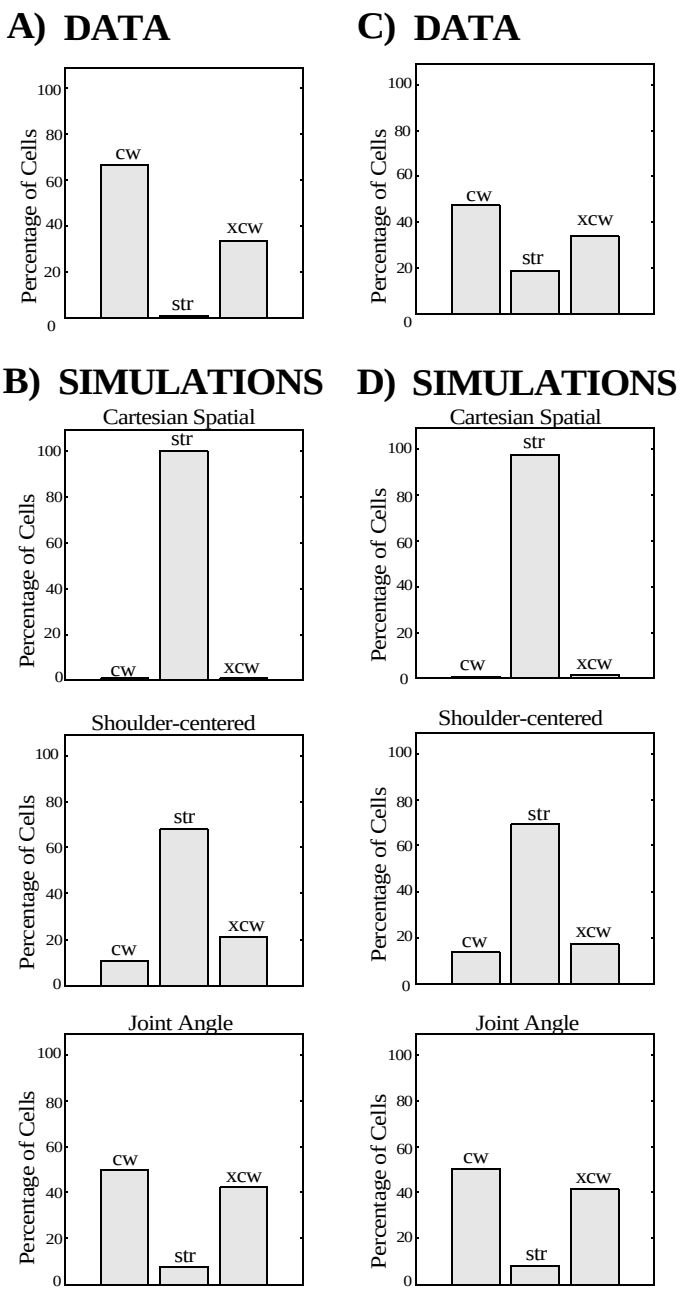

Figure 3. Plot of the percentages of cells trajectory-selective for each trajectory type using the strict criterion for cell classification as found in A) the data of Hocherman and Wise (1991) (adapted with permission), and B) model simulations using each of the three internal coordinate systems. 'cw' stands for clockwise trajectory-selective, 'str' stands for straight trajectory-selective, and 'xcw' stands for counter-clockwise trajectory-selective. Note that in the data all cells respond preferentially to the curved trajectories while, in the model simulations, most cells respond preferentially to the straight trajectories under the assumption of Cartesian spatial or shoulder-centered coordinates. Under the assumption of joint angle coordinates, the vast majority of model cells respond preferentially to the curved trajectories as in the data. C) and D) are analogous plots of data (adapted with permission) and model simulations, this time using the relaxed criterion for cell classification. Once again, a preponderance of cells in the data respond preferentially to the curved trajectories while the same is true in the model simulations only when joint angle coordinates are used.

To understand the simulation results, recall Equation 5. It implies that, over the course of a trajectory, a cell registers significant activity while the movement direction is parallel to the spatial pd; the greater the deviation from colinearity, the less the activity generated. The average firing rate of a cell for an entire movement, then, depends upon the interaction between the vector field structure of spatial pds and the sequence of movement directions taken by the hand. Previously, it was shown that the hypothesis of a particular coordinate system imparts a signature structure to the vector field of spatial pds. Similarly, each type of movement curvature (clockwise, straight, counter-clockwise) engenders its own characteristic pattern of movement directions. The movement direction for clockwise movements rotates continuously and in a clockwise manner from the beginning of the movement to its end for a net rotation of about $90°$. The reverse is true for the counter-clockwise movements. During straight movements, the movement direction never changes. The observed ratios of trajectory-selectivity for a given coordinate system can be understood by considering, within the context of

the task, how these characteristic movement patterns interact with each vector field structure.

For example, the spatial pds of vector fields generated by the assumption of joint angle coordinates tend to rotate in a uniform direction over the entire course of each trajectory. Figure 4 shows plots of a model cell's spatial pd values over the course of a clockwise trajectory and a straight trajectory to a particular target under the assumption of each coordinate system. It can be seen in the plot of the joint angle coordinate simulation that the spatial pd is not initially aligned with the movement direction at the beginning of the clockwise movement, but the two gradually fall into alignment over the course of the trajectory. The reverse is true for the straight trajectory.

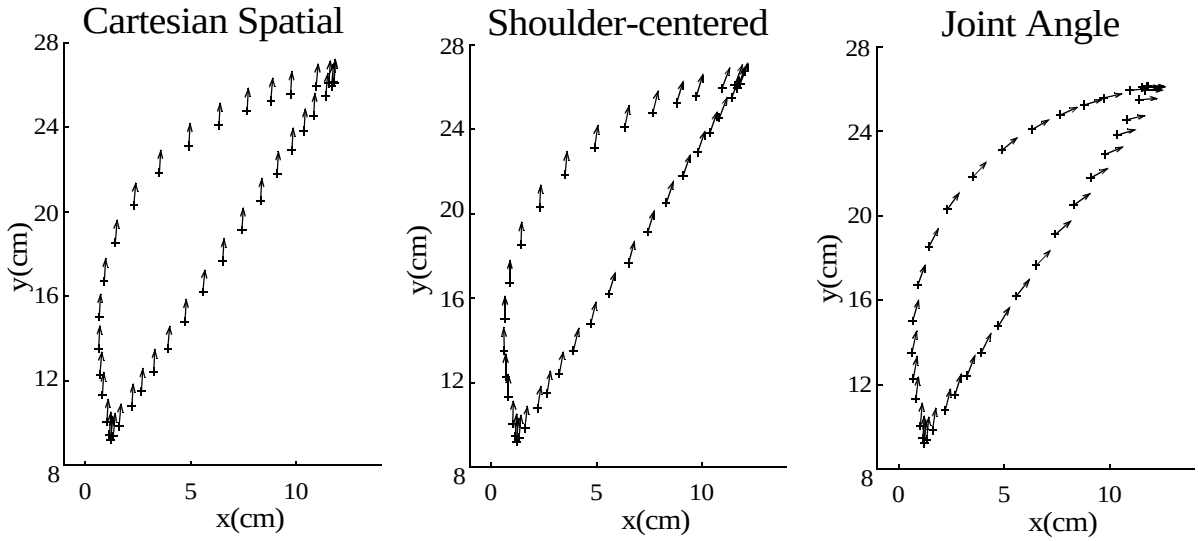

Figure 4. A cell's changing spatial pd over the course of a clockwise movement path and a straight movement path under the assumption of each internal coordinate system. Each arrow represents the cell's spatial pd at that point in the workspace. For the joint angle coordinate simulation, the spatial pd is initially out of alignment with the movement direction for the clockwise trajectory, but falls into alignment as the movement proceeds. This effect causes cells to respond preferentially to clockwise movements under the assumption of joint angle coordinates, making it clockwise trajectory-selective using the strict criterion for cell classification. The spatial pd for this cell is 86° at the reference posture, which was the origin of the simulated movement.

A rotating movement direction can engender considerable activity when paired with a rotating spatial pd if they rotate in the same direction and if the movement direction rotates more sharply, over the same spatial extent, than the spatial pd — a situation which does arise in the case of joint angle coordinates for the curved movements in this experiment. The dual rotation facilitates the occurrence of an interval of overlap during which the two directions are nearly aligned. At some point, the movement direction 'overtakes' the spatial pd although these directions may not be initially aligned, and this tendency toward alignment occurs for multiple movements of the same curvature type even when the final targets of these movements are different. Thus, the assumption of joint angle coordinates gives rise to relatively large proportions of cells that are trajectory-selective for the curved trajectory types. In contrast, under the assumption of either Cartesian spatial or shoulder-centered coordinates, there is either no tendency or a much weaker tendency for the spatial pds to rotate over the course of the trajectories, and what rotation does occur is often not unidirectional over an entire trajectory. This produces model cells that respond preferentially to straight trajectories.

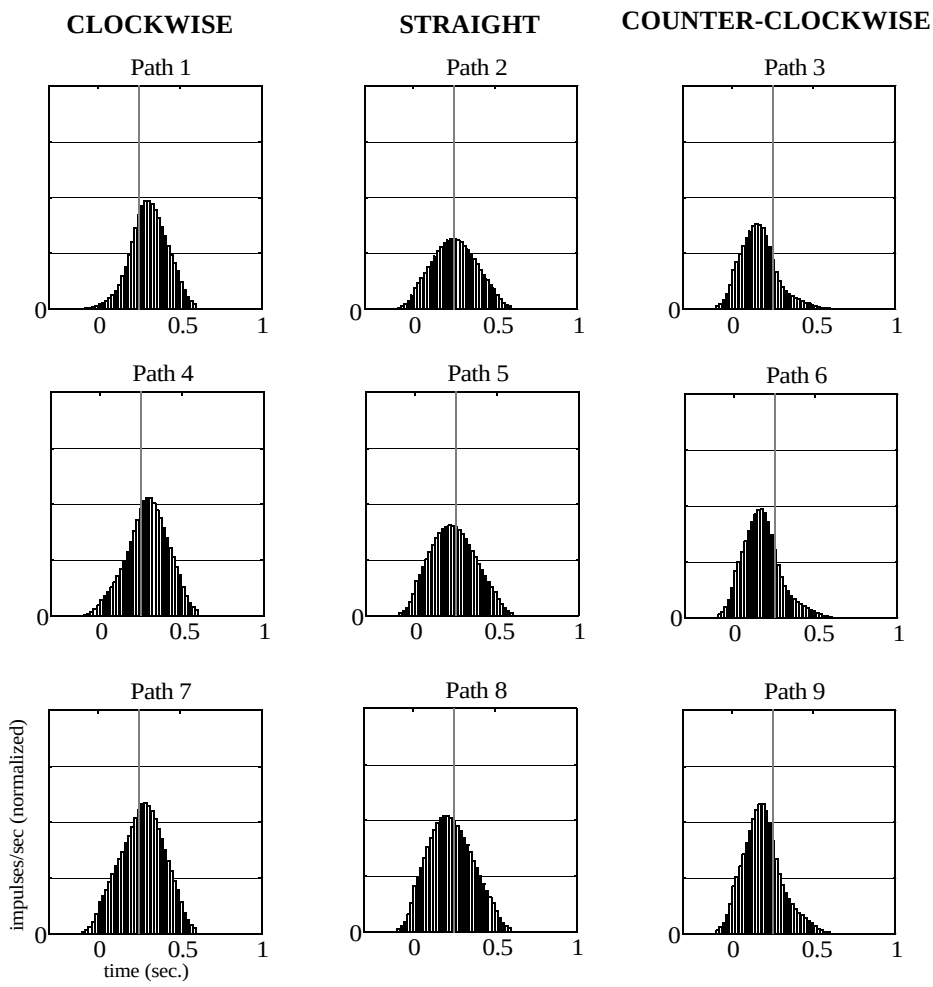

Figure 5. The temporal response profiles of a sample cell for each of the nine movement paths. The y-axis corresponds to cell activity in normalized units while the x-axis corresponds to time in seconds with the movement-related activity beginning at $t = 0$. The dashed vertical line in the middle of the figure corresponds to the midpoint of the movement-related interval at $t = 250$. Note that the peaks and total areas of the response profiles, as well as the timing of the peaks, vary characteristically depending upon the trajectory type. This cell is clockwise trajectory-selective (strict criterion) with a spatial pd of $36°$ at the reference posture. The profiles were generated by using the bin-wise cosine between the local trajectory direction and the spatial pd to multiply a Gaussian which reflects the phasic response properties of many MI cells.

Simulations of cell response profiles. In addition to simulating the average activity over the course of an entire trajectory, the model can also simulate, as shown in Figure 5, the temporal response profiles of a cell for each of the nine different movement trajectories under the assumption of joint angle coordinates. Figure 5 shows that cell response properties vary as a function of movement curvature. For example, the relative timing of peak activity depends critically upon the time-evolving relationship between the hand's movement direction and the cell's spatial pd for the movement path under consideration. The peak activity for the model cell occurs 150-200 msec after the onset of movement-related activity for the counter-clockwise movement paths and 275-325 after onset for the clockwise movement paths. This predicted time lag between the peak activities can be tested experimentally. Such temporal differences in activity profiles exist for all the response envelopes we tried since these differences stem from the variable directional component of cellular response, which is highly differentiated in this paradigm as a function of curvature type. For other model cells (depending upon the spatial pd at the reference posture), the relative timing of peak activity as a function of movement curvature will be reversed: the peak activity will occur sooner for the clockwise paths than for the counter-clockwise paths.

This cell is typical of all model cells in two important respects: 1) its response characteristics — such as its peak firing rate, mean firing rate, and the timing of its peak firing rate — change

relatively gradually from one trajectory type to the next; and 2) the mean activity levels across trajectory types are ordered in a characteristic manner — i.e., a clockwise trajectory-selective cell will be most active for the clockwise paths, least active for the counter-clockwise paths, and intermediately active for the straight movement paths (the inequality is reversed for counter-clockwise trajectory-selective cells). In what follows, we analyze Hocherman and Wise (1991) data with respect to the above two model cell response properties.

Comparison of model cell response properties with data. Do real MI cells exhibit graded responses such as those illustrated in Figure 5? Instead, an MI cell might be highly modulated for clockwise trajectories but relatively silent for straight and counter-clockwise movements. If curvature were explicitly encoded as a movement primitive by MI cells, then one might expect such a discretization of response characteristics. Some of the plotted response profiles in Hocherman and Wise (1991) seem to support the all-or-none view, although this type of analysis was not performed in that study. To assess whether MI cell activity more closely conforms to the graded or categorical response characteristics, we obtained the original data files for 59 of the 76 task-related MI neurons (which included 19 of the 24 trajectory-selective cells using the strict criterion) from Hocherman and Wise (1991) and analyzed the spread in activity for movements of different curvature types. Specifically, for each trajectory-selective cell, let $\bar{A}_{cw}$, $\bar{A}_{xcw}$, and $\bar{A}_{str}$ denote cell activity averaged over each set, respectively, of clockwise movements, counter-clockwise movements, and straight movements. For example, $\bar{A}_{cw}$ denotes cell activity averaged over the clockwise movement paths 1, 4, and 7 in Figure 2. Consequently, a separation index, analogous to the modulation index, was defined for each trajectory-selective cell as:

$$\frac{A_{max} - A_{min}}{A_{MAX} - R}, \tag{7}$$

where A_{max} is the largest of $\bar{A}_{cw}$, $\bar{A}_{xcw}$, and $\bar{A}_{str}$; A_{min} is the least of these three averages; A_{MAX} is the cell's average discharge rate over that movement path (of the nine) for which the cell is maximally active; and R is the cell's resting discharge rate. The numerator represents the absolute spread in activity as a function of curvature type while the denominator represents the maximum amount of movement-related activity exhibited by the cell. The ratio can range from 0 to 1 with a fraction close to 1 suggesting that the curvature-dependent activity possesses close to an all-or-none character, while a fraction close to 0 suggests that activity varies rather gradually as a function of movement curvature.

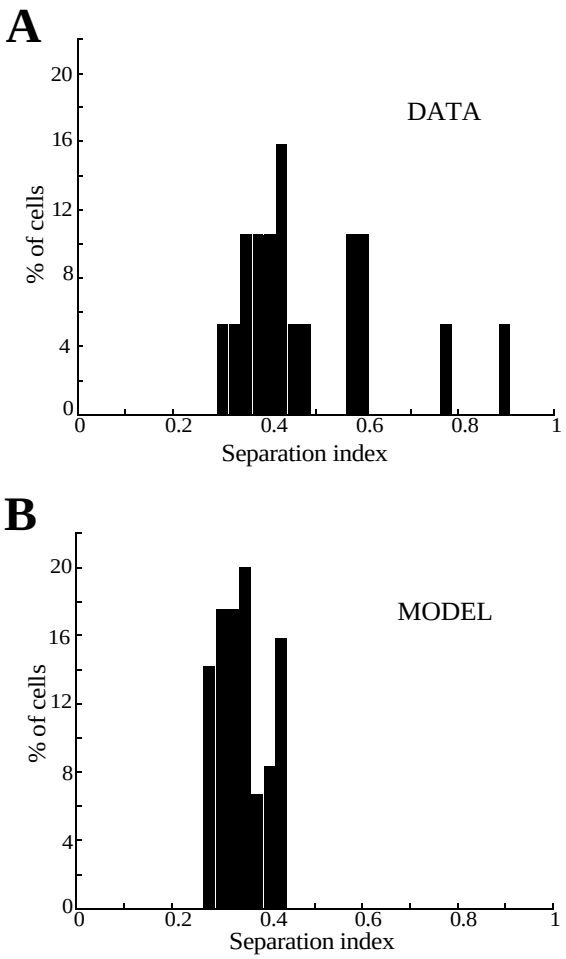

Figure 6. A) Plot of the distribution of the separation indices for the trajectory-selective cells in the experiment of Hocherman and Wise (1991). B) Same plot constructed for model cells. For both plots, the indices of separation are clustered below 0.5. This indicates that cell response varies relatively gradually as a function of movement curvature in both the data and the model. All or none coding of curvature would yield values closer to 1 (the maximum possible).

Figure 6A plots the distribution of separation indices for the population of trajectory-selective cells in Hocherman and Wise (1991). The mean and median separation indices are 0.48 and 0.43, suggesting that (outside of the small percentage of outliers present in the plot) cell response varies relatively gradually as a function of movement curvature. Figure 6B plots the corresponding distribution of simulated separation indices for the population of model trajectory-selective cells under the assumption of joint angle coordinates. The mean and median separation indices are 0.35 and 0.34. Note that for both distributions the vast majority of separation indices lie in the interval between 0.3 and 0.5. Therefore, the gradual variation exemplified by the Figure 5 model cell is a characteristic feature of both the model and the dataA second distinctive feature of model cell response properties is the very specific ordering of mean activity as a function of curvature type. In particular, for every clockwise trajectory-selective model cell, the following condition holds: $\bar{A}_{cw} > \bar{A}_{str} > \bar{A}_{xcw}$. This condition (with the inequality accordingly reversed) also holds for every counter-clockwise trajectory-selective model cell. For the population of curved trajectory-selective cells in Hocherman and Wise (1991), 89% of the cells (17/19) showed the same ordering in their activity. Thus, the model reproduces not only the observed graded responses, but also the observed ordering of those responses.

Varying simulation parameters. There are no free parameters in the model, since the only model variable is a cell's vector field of spatial pds, which is completely determined as a function of the working coordinate hypothesis. However, the simulations did require values for the location of the movement origin, the speed profiles of the hand, the lengths of the arm segments, and b_0 and b_1 of a cell's tuning curve. Regarding the kinematic movement parameters, Hocherman and Wise (1991) did not have precise measurements for these quantities. Therefore, while the values used in the simulations were in accord with the specifications communicated to us by Dr. Wise, we systematically varied these parameters to probe the robustness of the results regarding trajectory-selectivity. The Appendix provides the details of these sensitivity analyses, the findings of which demonstrate the robustness of the simulation results for all three coordinate systems. Varying the cellular parameters b_0 and b_1 (which must be assumed since no center-out task is performed to determine them in Hocherman and Wise, 1991) did not alter a cell's trajec-

tory-selectivity as shown in the Appendix. The use of response envelopes with different pulse functions or with the constant function made no significant difference in the simulation results. Finally, although the simulations employed a uniform distribution of spatial pds at the reference posture (as revealed in Lurito et al. 1991), distributional skewing away from non-uniformity, such as that reported in the literature (Georgopoulos et al. 1982; Scott and Kalaska 1997) did not change the character of the results under the assumption of any of the three internal coordinate systems.

Amplitude effects. In the experiment of Hocherman and Wise (1991), the curved paths were longer than the straight paths (23 cm as opposed to 20 cm) so the prevalence of curved trajectory selective cells could conceivably result from an amplitude-dependence of the cell firing function (Fu et al. 1993, 1995). However, this hypothesis conflicts with the observed ordering of cell activity by trajectory type which indicates that, for the actual clockwise trajectory cells, $\bar{A}_{cw} > \bar{A}_{str} > \bar{A}_{xcw}$ (the order of inequalities is reversed for counter-clockwise trajectory selectivity). Even if modulation indices are scaled outright by path length, the simulation results for Cartesian spatial and shoulder-centered coordinates grossly contradict this observed ordering.

The effect of other movement variables. We conducted analyses (see Appendix) to assess whether a simple dependence of cell firing rates on either hand speed or hand position could alter the relative goodness of fit of the three coordinate hypotheses. The inclusion of these correlations did not change the nature of the results. The joint angle coordinate hypothesis continued to fit the data well while the other two coordinate systems failed. Although we believe that amplitude and hand speed were the most pertinent task variables (aside from direction) to consider in explaining the data, these variables comprise only a subset of the known correlates of MI cell activity (see Introduction). Additional studies would be needed to assess whether correlations with other movement-related variables could provide an alternative or supplementary explanation of the Hocherman and Wise (1991) data.

Prediction: internal pd controls spatial pd and trajectory-selectivity. The simulations of the Hocherman and Wise (1991) experiment not only determine the percentages of cells selective for the different trajectory types but also imply a relationship between a cell's internal pd and its trajectory-selectivity. Specifically, a cell's spatial pd at a reference posture maps to a cell's internal pd; from the cell's internal pd, a vector field of spatial pds is generated; from the cell's vector field of spatial pds, the cell's trajectory-selectivity is determined. Thus, a mapping is constructed from the spatial pd of a cell at a reference posture to the type of trajectory-selectivity which that cell is predicted to possess. For example, a model cell with a spatial pd of $45°$ at the reference posture is clockwise trajectory-selective under the assumption of joint angle coordinates. Table 1 depicts the complete predicted mapping from a cell's spatial pd at the reference posture to its trajectory-selectivity using the example of joint angle coordinates. This prediction can be tested in an experiment that determines both spatial pds through the center-out task and cellular trajectory-selectivity through the curved motion task of Hocherman and Wise (1991). The end result of this composite protocol would be an empirical determination of the mapping between spatial pds at the reference posture and type of trajectory-selectivity. Model mappings constructed for each internal coordinate system could then be compared with the actual mapping to assess the goodness of fit of alternative coordinate hypotheses.

Target selectivity. In addition to classifying cells as trajectory selective, Hocherman and Wise (1991) classified cells as target selective if the cells responded preferentially to movements to a specific target as compared with the responses to movements to the other targets. For the purpose

of representing the findings of Hocherman and Wise (1991) on target selectivity and of showing corresponding simulation results (using the strict criterion of classification), let x/y/z indicate that x% of task-related cells are target selective for target #1, y% of cells are target selective for target #2, and z% are target selective for target #3. On the basis of Table 3 and Figure 12b in their paper, the percentages of excitatory target selective cells found by Hocherman and Wise (1991) were 42/29/29. For the Cartesian spatial simulations, the percentages were 33/31/36; for the shoulder-centered simulations, the percentages were 38/16/46; for joint angle simulations, the percentages were 46/16/38. Thus, all three coordinate hypotheses roughly reproduce the results on target selectivity, and these target selectivity data cannot distinguish between coordinate systems**.**

Table 1: **Prediction**

Spatial pd of a model cell at the reference posture (in degrees)	Predicted trajectory-selectivity
27 - 91	clockwise
92 - 95	indeterminate
96 - 105	straight
106	indeterminate
107 - 161	counter-clockwise

Table 1. Predicted results for a composite protocol that conjoins the standard center-out task (Georgopoulos et al., 1982) and the curved motion task of Hocherman and Wise (1991) under the assumption of joint angle coordinates. The center-out task will determine a cell's spatial pd at a reference posture. The curved motion task will result in a cell's being either 1) trajectory-selective for either the clockwise, straight, or counter-clockwise trajectory type (using the strict criterion of cell classification), or 2) indeterminate trajectory-selective, which means that the cell is modulated by the task but cannot be classified as responding preferentially to one of the three movement types using the strict criterion (for example, the cell may respond preferentially to the clockwise movement for Target A but responds preferentially to the straight movement for Target B). Those cells absent from the list are not found to be task-related. The table above maps the dual experimental outcomes to each other on a cell by cell basis implicitly utilizing a cell's assumed internal pd as the common underlying factor (and sole cellular response characteristic) in generating cell behavior for each paradigm. As this experiment has not been performed, these simulation results serve as an untested prediction, the confirmation of which would provide further support for the contention that observed results on cellular trajectory-selectivity (Hocherman and Wise, 1991) are derived from joint angle directional control and not from the explicit encoding of curvature as a movement primitive or from the encoding of other movement variables.

Compatibility of joint angle coordinates with prior population vector analyses. The population vector algorithm (PVA) has been used to predict movement direction over the course of a trajectory on a bin-by-bin basis with good results (for review, see Georgopoulos, 1995). In standard use of the algorithm, the assumed spatial pds do not change as the hand moves from one bin to the next. If spatial pds in actuality do vary across the workspace, the population vector should rotate away from the movement direction as the movement progresses away from the point at which the cell's pd was assessed. Such a mismatch between the population vector direction and the movement direction would arise because the algorithm's invariant representation of the vectorial con-

tribution of each cell comes to lie in a direction slightly askew from each cell's actual preferred direction. Nonetheless, the very robustness of the PVA, as an aggregate estimator of movement direction, renders it insensitive to alternative coordinate assumptions (Mussa-Ivaldi, 1988; Sanger, 1994; Georgopoulos, 1996). To assess sensitivity in the current case, we performed a bin-by-bin population vector simulation for all eight movements in the standard center-out task. In this PVA, computed cell activity was based on the bin(posture)-dependent spatial pds determined by the joint angle coordinate model. The trajectories were divided into 25 bins each of length 20 msec. Under these conditions, the population vector did rotate away from the actual movement direction (due to the structure of the joint angle coordinate system), but the rotation was modest and the resultant prediction error was within the range of prior reports that used the PVA. The average amount of rotation from the beginning of a trajectory to the end of the trajectory was less than 10 degrees. Further, the mean absolute difference between the population vector direction and the movement vector direction over all of the bins was less than 5 degrees. That the mean signed difference was 0 degrees indicates the difficulty of utilizing a population vector analysis to distinguish between coordinate systems. Thus, the joint angle coordinate hypothesis is consistent with prior PVA results.

DISCUSSION

This paper presents a framework for analyzing the coordinate system in which an individual cell encodes movement direction. A cell's preferred direction can be predicted to vary across the workspace in a distinct manner depending upon the assumed internal coordinate system, and direct sampling experiments can be designed to probe these variations. Indirect sampling experiments examining cell activity over long, curved movements implicitly sample vector fields of spatial pds and can be used to choose between alternative coordinate hypotheses from the pattern of path-dependent activity. We simulated one such experiment (Hocherman and Wise 1991) under the assumption of three kinematic coordinate systems — Cartesian spatial, shoulder-centered, and joint angle — and found that joint angle coordinates robustly fit the MI data better than either of the other two coordinate systems.

These results do not imply that all MI cells encode movement direction in joint angle coordinates. First, only three coordinate systems were tested, and there may exist another coordinate system which fits the data better than joint angle coordinates. Second, even if a majority of cells within a given brain region represent movement direction in one particular coordinate system, evidence (Crutcher and Alexander 1990) suggests that there will often exist other cells in the same brain region which utilize different coordinate representations. Third, a recent investigation (Wise et al. 1998) demonstrates the capacity of motor cortex to rapidly reorganize its response properties during adaptation to a series of differentiated visuomotor tasks, perhaps implying that the central nervous system solves motor control problems by implementing task-specific solutions which utilize task-dependent coordinate decompositions of the sensorimotor transformation. Finally, the current analysis focuses on the representation of movement direction but, as reiterated above, cell activity likely reflects information about other movement variables as well. A more detailed exploration of the functional dependence of cell activity on multiple movement variables is warranted for clarifying these and other data.

By looking at the coordinate system in which an individual cell encodes movement direction, it becomes possible to assess how populations of cells with similar coordinate representations are distributed across a cortical area. Hocherman and Wise (1991) recorded in the supplementary motor area (SMA), dorsal premotor cortex (PMd), and ventral premotor cortex

(PMv) as well as MI. In these other cortical regions, a smaller percentage of cells responded preferentially to curved movements. From the present analysis we infer that MI represents movement commands in a coordinate system possessing a stronger joint angle character than do the SMA, PMd, or PMv. This conclusion is consistent with the findings of Scott et al. (1997).

Our study uses curved movements as a means to probe the structure of a cell's vector field of spatial pds by indirectly sampling the workspace. Another way to investigate vector field structure is by *directly* sampling the workspace, and two prior studies involving proximal arm movements fall into that category: Caminiti et al. (1990) and Scott and Kalaska (1997). In Caminiti et al. (1990), a 3-D center-out task was performed from three distinct movement origins that were colinear (normal to the saggital plane), spaced 10 cm apart, and situated in a transverse plane cutting through the shoulders. Spatial pds were found to change across the workspace by a statistically significant amount. These changes were fit reasonably well by assuming that the change in a cell's spatial pd matches the rotation of the shoulder joint from one workspace location to the next. Since the rotation of the shoulder joint from one workspace location to the next, proceeding from left to right, is virtually equivalent in this task to the rotation of the shoulder-hand axis ($18°$ and $20°$ for the former as opposed to $21.8°$ and $21.8°$ for the latter), the shoulder-centered coordinates defined in this paper would fit the data about as well. Lacking information regarding the movement trajectories in joint angle space (which is here necessary since an unconstrained arm operating in 3-D space is motor redundant), we were unable to simulate this paradigm under the assumption of joint angle coordinates.

In Scott and Kalaska (1997), a monkey performed the center-out task in two different postures (natural and abducted) which corresponded to the same end-effector location in space. They noted a significant posture by direction interaction effect present in the response properties of a majority of cells and demonstrated statistically that changes in a cell's directional preference were a major contributing factor. The difference between the mean spatial pds across the two arm orientations was significant for 48% of the 422 cells examined. Scott and Kalaska (1997) modeled these data using Cartesian spatial, joint angle, and joint torque coordinate systems. They found that joint angle coordinates best fit the data. The results were incompatible with the assumption of either Cartesian spatial or shoulder-centered coordinates.

On the basis of our analyses as well as the analyses in Caminiti et al. (1990) and Scott and Kalaska (1997), Table 2 provides an evaluation of the adequacy of the three different coordinate systems modeled in this paper with regard to three experiments, each of which investigated proximal arm cell activity during unloaded reaching movements: Caminiti et al. (1990), Hocherman and Wise (1991), and Scott and Kalaska (1997).

Table 2: Summary evaluation

	Caminiti et al. (1990)	**Scott and Kalaska (1997)**	**Hocherman and Wise (1991)**
Cartesian spatial	inconsistent	inconsistent	inconsistent
Shoulder-centered	consistent	inconsistent	inconsistent
Joint angle	untested	consistent	consistent

Table 2: A summary evaluation of each coordinate system with regard to each of three experiments involving

unloaded planar arm movements.

The observations of Caminiti et al. (1990) and Scott and Kalaska (1997) may appear to contradict the findings of Schwartz (1992), which investigated the temporal discharge patterns of individual cells in motor cortex during the tracing of sinusoids. It was found that cell discharge patterns correspond closely (high correlation coefficient) to what would be predicted under the assumption of a fixed spatial pd (i.e., Cartesian spatial coordinates), once the time lag between the cortical signal and its controlling effect at the periphery is taken into account. One could conceivably interpret these findings as support for Cartesian spatial coordinates, although Schwartz (1992) does not address the issue of coordinate systems and makes no claims in this regard. The framework for coordinate analysis established in this paper suggests that the results of Schwartz (1992) do not support or refute any coordinate system hypothesis. Differentiating between coordinate systems requires (1) probing the organization of spatial pds across a broad postural range that includes both the central and peripheral portions of the workspace, and (2) comparing the results with those predicted by alternative coordinate systems. The height of the sinusoids in Schwartz (1992) ranged from 3-12 cm and their horizontal extent was roughly 15.5 cm. Although detailed postural information was not given, the dimensions, location, and orientation of the 2-D workspace indicate that the monkeys were able to trace the sinusoids without moving the contributing joints through more than a relatively small fraction of their full range of motion. Such was not the case in Caminiti et al. (1990) or Hocherman and Wise (1991), where the larger dimensions of the workspace ($30\,\text{cm} \times 10\,\text{cm} \times 10\,\text{cm}$ and $20\,\text{cm} \times 20\,\text{cm}$ respectively) required a broader range of joint angles that would make changes in a cell's spatial pd more easily discernible.

Spatial pds will not vary significantly over small postural changes under *any* of the three considered coordinate systems, so it is not surprising that Cartesian spatial coordinates engendered good correlations in Schwartz (1992). Further, a definitive analysis must compare correlations under the assumption of Cartesian spatial coordinates vs. correlations under the assumption of alternative coordinate systems. Such comparisons are as important as broad workspace sampling and without them, one cannot make strong inferences about coordinate systems.

Although our analysis has focused on proximal arm movements, the approach can also be applied to the investigation of distal movements. Kakei et al. (1999) performed a direct sampling experiment on movements restricted to the wrist and hand. Preferred directions of MI cells during a latency interval (final 100 msec. before movement onset) were determined in three different wrist postures: pronated, supinated, and midway between pronated and supinated. On the basis of the relative size of posture-dependent shifts in cellular pds, Kakei et al. (1999) divided the population into a class of "muscle-like" (sizeable pd shift) cells (32%) and a larger class of "extrinsic-like" (limited pd shift) cells (50%). At least two considerations argue for being cautious in treating these "extrinsic-like" cells as truly extrinsic. First, roughly 60% of extrinsic-like cells exhibited large posture-dependent gain changes, a response feature analogously found in muscle activations but not expected of a true extrinsic coding scheme. Second, as shown by Scott and Kalaska (1997) and by our simulations, not all cells that encode direction in a purely intrinsic coordinate system will exhibit significant shifts in their pds: it depends upon the specific internal pd. More research is needed to clarify the implications of these important results.

The generality of the vector field framework makes it applicable to all well-defined coordinate frames, including kinematic, kinetic, and hybrid kinematic-kinetic frames. For example, a plausible hypothesis is that motor cortical cell activity reflects combinations of muscle shortening rates (Mussa-Ivaldi 1988). Support for the idea of bound muscle synergies comes from post-spike

facilitation studies (Fetz et al. 1976, 1978, 1980) which suggest that motor cortical cells typically project to motor neurons associated with more than one muscle. Generating predictions for muscle-length coordinates requires a detailed biomechanical model of the arm-muscle system and knowledge of the recruitment patterns by which multiple muscles are synergistically innervated by individual cortical cells. Extending the framework to consider a kinetic, muscle-force based coordinate system remains desirable, particularly for MI, because muscle forces ultimately drive movements and because anatomical and physiological considerations have long shown MI to provide prominent cortical input to the spinal cord and motoneurons. Studies have established correlations between MI cell activity and force for multijoint movements (Kalaska et al. 1989; Bullock et al. 1998; Sergio and Kalaska 1998). Unfortunately, an analysis of a muscle force coordinate system would require, in addition to a detailed biomechanical model and knowledge of cortical recruitment patterns, an understanding of all relevant elastic, inertial, and viscous forces involved in center-out hand movements. Given the difficulty in gauging these forces — which are intricately composed, highly complex, and posture-dependent — reliably constructing an explicit muscle-force based coordinate system is an exceedingly difficult task. While we did not attempt to model such a coordinate system, skeletomuscular considerations suggest that a vector field of spatial pds based on muscle forces would possess a highly curved structure. A more efficacious analysis of kinetic coordinate systems can be achieved by applying the vector field framework to an analysis of postural variations of a cell's preferred direction of force in isometric tasks (Sergio and Kalaska 1997). Finally, the framework can be extended to the analysis of a system of non-canonical coordinates defined by a set of motor primitives like those proposed by Bizzi et al. (1991) to explain the results of stimulating intermediate grey matter in the spinal frog. If a cell controls a fixed linear combination of these force fields, a vector field of spatial pds which represents either movement directions or force directions can, in theory, be constructed and subsequently evaluated in either movement or isometric tasks.

APPENDIX

Joint angle coordinate vector fields of spatial pds

The forward and inverse kinematic equations of a 2-DOF planar arm are:

$$x = k_1\cos(\theta) + k_2\cos(\theta + \varphi) \tag{A1}$$

$$y = k_1\sin(\theta) + k_2\sin(\theta + \varphi) \tag{A2}$$

$$\theta = \operatorname{atan}\left(\frac{y}{x}\right) - \operatorname{acos}\left(\frac{r^2 + k_1^2 + k_2^2}{2k_1 r}\right) \tag{A3}$$

$$\varphi = \operatorname{acos}\left(\frac{r^2 - k_1^2 - k_2^2}{2k_1 k_2}\right) \tag{A4}$$

where $r = \sqrt{x^2 + y^2}$. The forward Jacobian (joint angle velocities to end-point velocities) is: The inverse Jacobian is:

$$\mathbf{J}^{-1}(\theta, \varphi) = \frac{1}{k_1 k_2 \sin\varphi}\begin{pmatrix} k_2\cos(\theta + \varphi) & k_2\sin(\theta + \varphi) \\ -k_1\cos(\theta) - k_2\cos(\theta + \varphi) & -k_1\sin(\theta) - k_2\sin(\theta + \varphi) \end{pmatrix} \tag{A6}$$

Suppose the spatial pd of a cell at a reference posture of (θ_R, φ_R) is ω_{pd}. This direction can be recast as a cartesian velocity vector of the form $[\cos\omega_{pd}, \sin\omega_{pd}]^T$ which, when multiplied by

$$\mathbf{J}(\theta, \varphi) = \begin{pmatrix} -k_1 \sin(\theta) - k_2 \sin(\theta + \varphi) & -k_2 \sin(\theta + \varphi) \\ k_1 \cos(\theta) + k_2 \cos(\theta + \varphi) & k_2 \cos(\theta + \varphi) \end{pmatrix} \quad \text{(A5}$$

$\mathbf{J}^{-1}(\theta_R, \varphi_R)$, yields the internal pd, $[\dot{\theta}_{pd}, \dot{\varphi}_{pd}]^T$, that corresponds to a velocity vector in joint angle space. Let this joint synergy be normalized in joint angle space as $[\dot{\theta}^*_{pd}, \dot{\varphi}^*_{pd}]^T$. The corresponding vector field of spatial pds is constructed as:

$$\begin{pmatrix} v_x(\theta, \varphi) \\ v_y(\theta, \varphi) \end{pmatrix} = \mathbf{J}(\theta, \varphi) \begin{pmatrix} \dot{\theta}^*_{pd} \\ \dot{\varphi}^*_{pd} \end{pmatrix} \quad \text{(A7)}$$

by letting θ and φ vary across their allowable range of values. When the expression for the Jacobian shown in Equation A5 is plugged in, Equation A6 expands to:

$$\begin{pmatrix} v_x(\theta, \varphi) \\ v_y(\theta, \varphi) \end{pmatrix} = \begin{pmatrix} \dot{\theta}^*_{pd} \, [-k_1 \sin(\theta) - k_2 \sin(\theta + \varphi)] + \dot{\varphi}^*_{pd} \, [-k_2 \sin(\theta + \varphi)] \\ \dot{\theta}^*_{pd} \, [k_1 \cos(\theta) + k_2 \cos(\theta + \varphi)] + \dot{\varphi}^*_{pd} \, [k_2 \cos(\theta + \varphi)] \end{pmatrix}. \quad \text{(A8)}$$

Substitution of Equations A1 and A2 reduce Equation A8 to:

$$\begin{pmatrix} v_x(\theta, \varphi) \\ v_y(\theta, \varphi) \end{pmatrix} = \begin{pmatrix} \dot{\theta}^*_{pd} \, [-y] + \dot{\varphi}^*_{pd} \, [k_1 \sin\theta - y] \\ \dot{\theta}^*_{pd} \, [x] + \dot{\varphi}^*_{pd} \, [x - k_1 \cos\theta] \end{pmatrix}. \quad \text{(A9)}$$

Using the chain rule to compute the difference of partials that comprises the curl $\left(\frac{\partial v_y}{\partial x} - \frac{\partial v_x}{\partial y}\right)$ yields:

$$\text{curl } \mathbf{v} = \dot{\theta}^*_{pd} \, [2] + \dot{\varphi}^*_{pd} \left[2 + k_1 \left(\sin(\theta) \frac{\partial \theta}{\partial x} - \cos(\theta) \frac{\partial \theta}{\partial y}\right)\right]. \quad \text{(A10)}$$

These partial derivatives, rather than being explicitly computed, can be taken directly from the first row of the inverse Jacobian to produce:

$$\text{curl } \mathbf{v} = \dot{\theta}^*_{pd} \, [2] + \dot{\varphi}^*_{pd} \left[2 + k_1 k_2 \left(\frac{\sin(\theta)\cos(\theta + \varphi) - \cos(\theta)\sin(\theta + \varphi)}{k_1 k_2 \sin\varphi}\right)\right]. \quad \text{(A11)}$$

The resulting expression can be simplified using the cosine angle addition formula to yield:

$$\text{curl } \mathbf{v} = 2 \dot{\theta}^*_{pd} + \dot{\varphi}^*_{pd}. \quad \text{(A12)}$$

Remarkably, all intermediate dependencies of the curl on hand position and arm posture cancel, leaving a final expression for the curl which does not depend on hand location or arm posture and instead depends only on the joint synergy to which the cell is tuned. Thus, the rotational tendency of vectors in such a vector field remains uniform across the workspace.

A Magnitudes of pd vectors

The magnitude of an internal pd vector is assumed to be constant and, for simplicity, normalized to size unity. The corresponding magnitudes of the spatial pd vectors at different postures depend on the scaling effect of the transformation between the internal space and external space. Under the assumption of Cartesian spatial coordinates, all spatial pds are of magnitude unity since the transformation is the identity transformation. Under the assumption of shoulder-centered coordinates, the magnitude of all spatial pds is again unity, since the transformation is a rotational transformation with no scaling effects. However, under the assumption of joint angle coordinates, the magnitudes of spatial pds vary since the Jacobian introduces posture-dependent scaling effects. A natural physiological interpretation of the relative magnitude of a spatial pd vector at a posture is the relative depth of modulation of the cell's tuning curve. Such variation in response modulation is treated in Ajemian et al. (1998). For present purposes, it sufficed (except in the calculation of the curl) to focus exclusively on the direction of the vectors.

B Shoulder-centered coordinate vector fields

The vector field of spatial pds generated under the assumption of an internal pd in this shoulder-centered coordinate system is:

$$\omega_{pd}(x, y) = \omega_{pd}(x_R, y_R) + \left[\operatorname{atan}\left(\frac{y}{x}\right) - \operatorname{atan}\left(\frac{y_R}{x_R}\right) \right], \tag{A1}$$

where $\operatorname{atan}\left(\frac{y}{x}\right)$ represents the orientation of the shoulder-hand axis at the desired posture and $\operatorname{atan}\left(\frac{y_R}{x_R}\right)$ represents the orientation of the shoulder-hand at the reference posture and the difference in arctans represents the rotation of the shoulder-hand axis between the two postures. Thus, Equation A1 says that the spatial pd at an arbitrary posture equals the spatial pd at the reference posture plus the amount of rotation of the shoulder-hand axis required to shift from the reference posture to the desired posture. Substituting in the values for the hand position at the reference posture given in Figure 1 yields:

$$\omega_{pd}(x, y) = \omega_{pd}(x_R, y_R) + \operatorname{atan}\left(\frac{y}{x}\right) - \frac{\pi}{2} \tag{A2}$$

which can be decomposed into its x and y vector field components, denoted v_x and v_y:

$$v_x = \cos\left(\omega_{pd}(x_R, y_R) + \operatorname{atan}\left(\frac{y}{x}\right) - \frac{\pi}{2} \right) \tag{A3}$$

$$v_y = \sin\left(\omega_{pd}(x_R, y_R) + \operatorname{atan}\left(\frac{y}{x}\right) - \frac{\pi}{2} \right) \tag{A4}$$

where $\pi/2 = \operatorname{atan}(y_R/x_R)$ for the reference posture of (0,16). Using the chain rule to compute the partial derivatives that comprise the curl $\left(\frac{\partial v_y}{\partial x} - \frac{\partial v_x}{\partial y}\right)$ leaves:

$$\operatorname{curl}(x, y) = \frac{1}{r}\left[-v_x\left(\frac{y}{r}\right) + v_y\left(\frac{x}{r}\right) \right] \tag{A5}$$

where $r = \sqrt{x^2 + y^2}$. Trigonometric substitutions and application of the cosine angle addition

formula simplify the above expression to produce:

$$\text{curl}(x, y) = -\frac{1}{r}\cos(\omega_{pd}(x_R, y_R)) \qquad \text{(A6)}$$

C Simulation details

A cell is classified as clockwise trajectory-selective, according to the *strict* criterion of cell classification (Hocherman and Wise 1991), if the following three conditions hold:

i) $M_1 > M_2$ and $M_1 > M_3$

ii) $M_4 > M_5$ and $M_4 > M_6$

iii) $M_7 > M_8$ and $M_7 > M_9$,

where M_j is defined by Equation 6. The definitions for straight and counter-clockwise trajectory-selectivity are analogous. Using their *relaxed* criterion for cell classification, only two of the above three conditions need to hold.

To model the clockwise curved paths, the following function was used as a template: $x = \frac{y^2}{20} - y$ for $0 \le y \le 20$ where x and y are the bases (in cm's) of a Cartesian coordinate system whose origin is the movement origin (not the shoulder). This template was rotated by $-32°$, $4.5°$, and $36°$ in modeling, respectively, paths 1, 4, and 7 as illustrated in Figure 2. The counter-clockwise paths were constructed as mirror images of the clockwise movement paths. Each movement was assumed to begin at $t = 0$ msec and end at $t = 500$ msec. Speed profiles for movement paths were taken to be Gaussians with a standard deviation of $1/(\sqrt{60})$ sec and centered at $t = 250$ msec. Twenty bins of equal temporal duration (25 msec) were used to divide the movement paths. In a Cartesian coordinate system centered at the shoulder, the location of the movement origin, in cm, was $(1.2, 9.2)$. The length of the upper and lower arm segments were taken to be 13.5 cm and 16.2 cm, respectively. All the above parameter values conform to specifications communicated to us by Dr. Steven Wise. Since movements were made with the left arm in Hocherman and Wise (1991), a 2-DOF planar left arm was used in the simulations.

In Equation 6, R is taken to be 15 impulses/sec and A_{max} is taken to be 27 impulses/sec which is derived from $\upsilon(\omega) = b_0 + b_1\cos(\omega - \omega_{pd})$ by letting $b_0 = 15$ and $b_1 = 12$ and assuming the cosine term is always one. A cell was classified as task-related if its modulation index was greater than 0.5 for any one of the nine movement paths. Additional simulations were run under a range (0.2 - 0.8) of thresholds for task-relatedness, and the results were very similar. The values of b_0 and b_1 chosen above conform to typical values reported in the literature. Since trajectory-selectivity is a comparative measure, and since these constants apply for all nine movement paths, the choices of R, b_0, and b_1 will not alter a task-related cell's trajectory-selectivity (although they can alter whether or not the cell is deemed task-related). Their values, however, need to be specified for the simulations of temporal response profiles which were constructed by scaling a cell's direction-dependent activity within a bin, as given by Equation 1, by a Gaussian function which embodies the phasic response properties demonstrated by many MI cells.

Although the simulation results presented used a Gaussian response envelope with a stan-

dard deviation of $1/(\sqrt{20})$ sec and centered at $t = 250$ msec, multiple response envelopes were tried including Gaussians of different standard deviations and centers as well as the constant function. As indicated in the Results, all methods gave very similar results regarding trajectory-selectivity and qualitative response characteristics (such as the relative timing of the peak activity for clockwise as opposed to counter-clockwise movement paths).

Model robustness was assessed by testing the sensitivity of simulation results to variations in the location of the movement origin, the lengths of the arm segments, and the shape of the velocity profile. For example, movement origins were scattered randomly in that area where the movement origin was most likely to lie based upon the estimates of Dr. Steven Wise. To vary the lengths of the arm segments, link lengths were incremented and decremented independently. To vary the shape of the velocity profile, Gaussians with different standard deviations were used. In summary, varying the parameters did not alter the finding that a clear majority of cells were preferentially active for the straight trajectories under the assumption of Cartesian spatial and shoulder-centered coordinates. The simulations were more sensitive (particularly to the relative lengths of the arm segments) under the assumption of joint angle coordinates, but there were always sizeable percentages of cells which responded preferentially to the curved trajectories. Therefore the main feature of the data — a preponderance of cells which are preferentially active for the curved trajectories as opposed to the straight ones — was robustly replicated by the model under the assumption of joint angle coordinates but was robustly absent when simulations were run using Cartesian spatial or shoulder-centered coordinates.

Several authors (Bullock et al. 1988, 1998; Mussa-Ivaldi 1988; Moran and Schwartz 1999; Zhang and Sejnowski 1999) have suggested that cell firing rates may depend on the product of a directional component with a velocity component. A slight change to Equation 1 yields:

$$\upsilon(\alpha) = b_0 + b_1|v|\cos(\omega - \omega_{pd}), \qquad \text{(A7)}$$

where $|v|$ denotes the instantaneous hand speed.

In Equation A7, the cosine term in Equation 1 is multiplied by $|v|$. This speed effect can be taken into account by scaling the activity of a cell within a given bin by the hand speed as revealed by the velocity profile. Although Hocherman and Wise (1991) did not record detailed velocity profiles, the speed effect can be approximated by scaling the simulated modulation index of each movement by the measured average speed of the corresponding real movement. Thus, faster movements (which in this experiment tended to be the movements of greater amplitude as well) will be associated with a higher level of activity than slower movements.

Additional simulations were run utilizing such speed scaling after the average movement speeds were computed (separately for the two monkeys in the experiment) by dividing each path length by the respective mean movement time required for traversal. To depict simulation results numerically, cw/str/xcw is taken to mean that cw% of the trajectory-selective cells are clockwise trajectory-selective, str% are straight trajectory-selective, and xcw% are counter-clockwise trajectory-selective. Under the assumption of Cartesian spatial coordinates, the trajectory-selective cells were split among the different curvature types as follows: 0/100/0 using the strict criterion and 30.3/69.7/0 using the relaxed criterion. Under the assumption of shoulder-centered coordinates, the corresponding percentages are 26.7/45.9/27.4 and 30.7/40.6/28.7. For both coordinate systems, straight trajectory-selectivity is the dominant cell type, and this finding contrasts sharply with the data. The simulations run using joint angle coordinates, however, did produce a distribution of trajectory-selective cells similar to that seen in the data: 57.9/4.2/37.9 and 54.8/6.1/39.1. Therefore, simple speed effects, divorced from joint angle directional encoding, do not explain

the key feature of the data but may contribute to such an explanation in conjunction with other factors.

To model positional dependence in concert with directional dependence, we used a composite model of instantaneous cell activity:

$$\upsilon = b_0 + k[b_1 \cos(\omega - \omega_{pd})] + [\alpha x + \beta y], \qquad \text{(A8)}$$

where the first term represents a baseline level of activity, the second term represents the direction-dependent cell modulation, and the third term represents the model of positional dependence outlined in Georgopoulos et al. (1984). A coefficient k is required to reflect the relative strength of the directional or dynamic component of cell activity as compared to the positional or static component. In Georgopoulos and Massey (1985), this coefficient in motor cortex is, on average, 1.51. In order to run the simulations, one also needs to know the correlation that exists between the preferred direction of a cell, ω_{pd}, and the preferred position direction; i.e., $\operatorname{atan}\frac{\beta}{\alpha}$. Georgopoulos and Massey (1985) indicate that for 26% of the cells, the spatial pd and the positional pd are positively correlated while for 15% of the cells, the two directions are negatively correlated. Therefore, for each simulation, which consisted of 360 cells (one per degree of the angular continuum corresponding to the cell's spatial pd), the positional pd was taken to be identical to the spatial pd for 26% of cells (chosen at random) while for 15% of the cells (also chosen at random), the directions are taken to be anti-parallel. The remainder of the cells were randomly assigned positional pds. One hundred such simulations were run, each with a new seed for the random number generator. Despite the element of randomness in matching up spatial pds with positional pds, it is noted that each simulation engendered qualitatively similar results. The average results on trajectory selectivity for the entire batch were as follows. Under the assumption of Cartesian spatial coordinates, the distribution of trajectory-selective cells is 23.9/53.9/22.2 for the strict criterion and 24.2/49.7/26.1 for the relaxed criterion. Under the assumption of shoulder-centered coordinates, the numbers are 18.7/60.4/20.9 and 12.5/69.1/18.4. In neither case does there exist a preponderance of cells preferring curved trajectories although such a preponderance characterizes the data. On the other hand, under the assumption of joint angle coordinates, a much better fit to the data is again achieved as the percentages of trajectory-selective cells are 53.7/14.8/31.5 and 41.9/27.3/30.8. Therefore, in the absence of joint angle directional coding, positional effects cannot explain the key feature in the data but may contribute to such an explanation in conjunction with other factors.

References

Ajemian, R., Bullock, D., and Grossberg, S. Computing single cell activity in motor cortex as a function of movement direction, hand speed, and intrinsic cellular coordinates. Soc. Neurosci. Abstr. 24: 1415, 1998.

Alexander, G.E., and Crutcher, M.D. Preparation for movement: neural representations of intended direction in three motor areas of the monkey. J. Neurophysiol. 64:133-150, 1990a.

Alexander, G.E., and Crutcher, M.D. Neural representations of the target (goal) of visually guided arm movements in three motor areas of monkey. J. Neurophysiol. 64:164-178, 1990b.

Ashe, J., and Georgopoulos, A.P. Movement parameters and neural activity in motor cortex and area 5. Cerebral Cortex 6:590-600, 1994.

Bizzi, E., Mussa-Ivaldi, F.A., and Giszter, S. Computations underlying the execution of movement: a biological perspective. Science 253:287-291, 1991.

Bullock, D., Cisek, P., and Grossberg, S. Cortical networks for control of voluntary arm movements under variable force conditions. Cerebral Cortex 8:48-62, 1998.

Bullock, D., and Grossberg, S. Neural dynamics of planned arm movements: emergent invariants and speed-accuracy properties during trajectory formation. Psychol. Rev. 95:49:90, 1988.

Caminiti, R., Johnson, P.B., Galli, C., Ferraina, S., and Burnod, Y. Making arm movements within different parts of space: The premotor and motor cortical representations of a coordinate system for reaching to visual targets. J. Neurosci. 11:1182-1197, 1991.

Caminiti, R., Johnson, P.B., and Urbano, A. Making arm movements within different parts of space: Dynamic aspects in the primate motor cortex. J. Neurosci. 10:2039-2058, 1990.

Carpenter, A.F., Georgopoulos, A.P., and Pellizzer, G. Motor cortical encoding of serial order in a context-recall task. Science 283:1752-1757, 1999.

Cheney, P.D., and Fetz, E.E. Functional classes of primate corticomotoneuronal cells and their relation to active force. J. Neurophysiol. 44:773-791, 1980.

Crutcher, M.D., and Alexander, G.E. Movement-Related Neuronal Activity Selectively Coding Either Direction or Muscle Pattern in Three Motor Areas of the Monkey J. Neurophysiol. 64:151-163, 1990.

Evarts, E.V. Relation of pyramidal tract activity to force exerted during voluntary movement. J. Neurophysiol. 31:14-27, 1968.

Fetz, E.E. Are movement parameters recognizably coded in the activity of single neurons? Behavioral and Brain Sciences 15:679-690, 1992.

Fetz, E.E., and Cheney, P.D. Muscle fields of primate corticomotoneuronal cells. J. Physiol. Paris 74:239-245, 1978.

Fetz, E.E., and Cheney, P.D. Postspike facilitation of forelimb muscle activity by primate corticomotoneuronal cell. J. Neurophysiol. 44:751-772, 1980.

Fetz, E.E., Cheney, P.D., and German, D.G. Corticomotoneuronal connections of precentral cells detected by post-spike averages of EMG activity in awake monkey. Brain Res. 114: 505-510, 1976.

Flanders, M., Tillery, S., and Soechting, J. Early stages in a sensorimotor transformation. Behavioral and Brain Sciences 15:309-362, 1992.

Fu, Q.-G., Flament, D., Coltz, J.D., and Ebner, T.J. Temporal encoding of movement kinematics in the discharge of primate primary motor and premotor neurons. J. Neurophysiol. 73:836-854, 1995.

Fu, Q.-G., Suarez, J.I., and Ebner, T.J. Neuronal specification of direction and distance during

reaching movements in the superior precentral premotor area and primary motor cortex of monkeys. J. Neurophysiol. 70:2097-2116, 1993.

Gandolfo, F., Mussa-Ivaldi, F.A., and Bizzi, E. Motor learning by field approximation. Proc. Nat. Acad. Sci. 93:3843-3846, 1996.

Georgopoulos, A.P. Current issues in directional motor control. Trends Neurosci. 18: 506-510, 1995.

Georgopoulos, A.P. Directional motor control: Reply. Trends Neurosci. 19: 138, 1996.

Georgopoulos, A.P., Ashe, J., Smyrnis, N., and Taira, M. The motor cortex and the coding of force. Science 256:1692-1695, 1992.

Georgopoulos, A.P., Caminiti, R., and Kalaska, J.F. Static spatial effects in motor cortex and area 5: Quantitative Relations in a two-dimensional space. Exp. Brain Res. 54:446-454, 1984.

Georgopoulos, A.P., Kalaska, J.F., Caminiti, R., and Massey, J.T. On the relations between the direction of two-dimensional arm movements and cell discharge in primate motor cortex. J. Neurosci. 2:1527-1537, 1982.

Georgopoulos, A.P., and Massey, J.T. Static versus dynamic effects in motor cortex and area 5: comparison during movement time. Behavioral Brain Res. 18:159-166, 1985.

Hocherman, S., and Wise, S.P. Effects of hand movement path on motor cortical activity in awake, behaving rhesus monkeys. Exp. Brain Res. 83:285-302, 1991.

Kakei, S., Hoffman, D.S., and Strick, P.L. Muscle and movement representations in the primary motor cortex. Science 285:2136-2139, 1999.

Kalaska, J.F., Cohen, D.A.D., Hyde, M.L., and Prud'homme, M. A comparison of movement direction-related versus load direction-related activity in primate motor cortex, using a two-dimensional reaching task. J. Neurosci. 9:2080-2102, 1989.

Kalaska, J.F., and Crammond, D.J. Cerebral cortical mechanisms of reaching movements. Science 255:1517-1523, 1992.

Kettner, R.E., and Marcario, J.K. Control of remembered reaching sequences in monkey. II. Storage and preparation before movement in motor and premotor cortex. Exp. Brain Res. 42:223-227, 1996.

Kettner, R.E., Schwartz, A.B., and Georgopoulos, A.P. Primate motor cortex and free arm movements to visual targets in three-dimensional space. III. Positional gradients and population coding of movement direction from various movement origins. J. Neurosci. 8:2938-2947, 1988.

Lacquaniti, F., Guigon, E., Bianchi, L., Ferraina, S., and Caminiti, R. Representing spatial information for limb movement: role of area 5 in the monkey. Cerebral Cortex 5:391-409, 1995.

Lurito, J.T., Georgakopoulos, T., and Georgopoulos, A.P. The making of movements at an angle from a stimulus direction: studies of motor cortical activity at the single cell and population levels. Exp. Brain Res. 87:562-580, 1991.

Maioli, C., and Lacquaniti, F. Posture and gait: Development, adaptation, and modulation. In: Determinants of postural control in cats: a biomechanical study. (B Amblard, A Berthoz and F Clarac, eds.) pp 371-379. Amsterdam: Elsevier Science Publishers, 1988.

Moran, D.W., and Schwartz, A.B. Motor cortical representation of speed and direction during reaching. J. Neurophysiol. 82: 2676-2692, 1999a.

Moran, D.W., and Schwartz, A.B. Motor cortical activity during drawing movements: population representation during spiral tracing. J. Neurophysiol. 82: 2693-2704, 1999b.

Morasso, P. Spatial control of arm movements. Exp. Brain Res. 42:223-227, 1981.

Mushiake, H., Inase, M., and Tanji, J. Neuronal activity in the primate premotor, supplementary, and precentral motor cortex during visually guided and internally determined sequential move-

ments. J. Neurophysiol. 66:705-718, 1991.

Mussa-Ivaldi, F.A. Do neurons in the motor cortex encode movement direction? An alternate hypothesis. Neurosci. Let. 91:106-111, 1988.

Pellizzer, G., Sargent, P., and Georgopoulos, A.P. Motor cortical activity in a context-recall task. Science 269:702-705, 1995.

Sanger, T.D. Theoretical considerations for the analysis of population coding in motor cortex. Neural Computation 6:29-37, 1994.

Schwartz, A.B. Motor cortical activity during drawing movements: Single unit activity during sinusoid tracing. J. Neurophysiol. 68:528-541, 1992.

Schwartz, A.B. Motor cortical activity during drawing movements: Population representation during sinusoid tracing. J. Neurophysiol. 70:28-36, 1993.

Schwartz, A.B. Direct cortical representation of drawing. Science 265:540-542, 1994.

Schwartz, A.B., Kettner, R.E., and Georgopoulos, A.P. Primate motor cortex and free arm movements to visual targets in 3-d space. I. Relations between single cell discharge and direction of movement. J. Neurosci. 8:2913-2927, 1988.

Sergio, L.E., and Kalaska, J.F. Systematic changes in directional tuning of motor cortex cell activity with hand location in the workspace during generation of static isometric forces in constant spatial directions. J. Neurophysiol. 78:1170-1174, 1997.

Sergio, L.E., and Kalaska, J.F. Changes in the temporal pattern of primary motor cortex activity in a directional isometric force versus limb movement task. J. Neurophysiol. 80:1577-1583, 1998.

Scott, S.H., and Kalaska, J.F. Reaching movements with similar hand paths but different arm orientations. I. Activity of individual cells in motor cortex. J. Neurophysiol. 77:826-852, 1997.

Scott, S.H., Sergio, L.E., and Kalaska, J.F. Reaching movements with similar hand paths but different arm orientations. II. Activity of individual cells in dorsal premotor cortex and parietal area 5. J. Neurophysiol. 78:2413-2426, 1997.

Shadmehr, R., and Mussa-Ivaldi, F.A. Adaptive representation of dynamics during learning of a motor task. J. Neurosci. 14:3208-3224, 1994.

Shen, L., and Alexander, G.E. Neural correlates of a spatial sensory-to-motor transformation in primary motor cortex. J. Neurophysiol. 77:826-852, 1997.

Soechting, J.F., and Flanders, M. Sensorimotor representation for pointing to targets in three-dimensional space. J. Neurophysiol. 62:582-594, 1989.

Tanaka, S. Hypothetical joint-related coordinate systems in which populations of motor cortical neurons code direction of voluntary arm movements. Neurosci. Let. 180:83-86, 1994.

Wise, S.P., Moody, S.L., Blomstrom, K.J., and Mitz, A.R. Changes in motor cortical activity during visuomotor adaptation. Exp. Brain Res. 121:285-289, 1998.

Zhang, K., and Sejnowski, T.J. A theory of geometric constraints on neural activity for natural three-dimensional movement. J. Neurosci. 19: 3122-3145, 1999.